Available online at www.sciencedirect.com
SCIENCE DIRECT®
Marine Geology 198 (2003) 5–25
MARINE GEOLOGY
INTERNATIONAL JOURNAL OF MARINE GEOLOGY, GEOCHEMISTRY AND GEOPHYSICS
www.elsevier.com/locate/margeo

A 3D seismic study of the morphology and spatial distribution of buried coral banks in the Porcupine Basin, SW of Ireland

V.A.I. Huvenne *, B. De Mol, J.-P. Henriet

Renard Centre of Marine Geology (RCMG), University of Ghent, Krijgslaan 281, S8, B-9000 Gent, Belgium

Accepted 13 February 2003

Abstract

An industrial 3D seismic data volume, supplemented by high-resolution 2D seismics, was used to study part of a province of buried mound structures in the Porcupine Basin, southwest of Ireland. These 'Magellan' mounds and their associated moat structures, interpreted as scour marks, were mapped semi-automatically from time-structure and isopach maps. Image analysis techniques such as a tophat transformation (mathematical morphology) were applied for feature extraction. Size measures of both mounds and moats were derived from the resulting maps and summarised by means of some descriptive statistics. Spatial variability in mound occurrence and characteristics was investigated. Comparison with other mound structures in the area allowed the Magellan mounds to be identified as 'coral banks', associated with the growth of cold-water deep-sea coral species such as *Lophelia pertusa* (L.) and *Madrepora oculata* (L.). Mound growth clearly started in a single 'event', confined in time and space. Bottom currents and oceanographic characteristics of the surrounding water masses influenced this sudden process and the further mound development. However, the analysis of the 3D seismic data set did not allow us to identify unambiguously the actual cause for the sudden mound start-up. The mounds appear to have formed a dense cluster of structures of moderate size, which are significantly elongated in a N–S direction. They are associated with even more elongated moats, implying a periodically reversing N–S-directed current influence. A spatial density of one mound per km^2 was measured, which remains more or less constant over the area investigated. Mound width and cross-sectional area and moat shape gradually change across the mound province, due to spatially changing environmental conditions at the initial growth stages of the mounds and during their further development (interplay between current regime and sedimentation).

Keywords: mounds; coral banks; tophat transformation; 3D seismics; Porcupine Basin

1. Introduction

The Porcupine Basin, southwest of Ireland, is a part of the NE Atlantic continental margin, bounded by the Porcupine Bank, Slyne Ridge, the Irish Shelf and Goban Spur (Fig. 1). It is a deep-seated, intracratonic extensional sedimentary basin which is the result of a Middle Jurassic failed rift (Shannon, 1991). Water depths range from 200 m at the shelf edge to more than 3500 m at the mouth of the Porcupine Seabight.

* Corresponding author. Tel.: +32-9-264-45-84; Fax: +32-9-264-49-67.
E-mail address: veerle.huvenne@rug.ac.be (V.A.I. Huvenne).

0025-3227/03/$ – see front matter © 2003 Elsevier Science B.V. All rights reserved.
doi:10.1016/S0025-3227(03)00092-6

Several processes affect the continental slope in this region: channel and canyon systems link the shelf edge with the abyssal plain (e.g. the Gollum Channel system; Kenyon et al., 1978; Tudhope and Scoffin, 1995); mass flows and submarine slope failures also cause downslope sediment transport (Moore and Shannon, 1991; Huvenne et al., in press). The alongslope sediment transport and/or (re)distribution is illustrated by contourite and drift deposits (Van Rooij et al., 2003). Processes closely linked to the general northward contour current (Pingree and Le Cann, 1989) and superimposed local current effects also affect the sediment dynamics. In some locations (e.g. Connemara field, Fig. 1) pockmarks occur at the seabed, while iceberg ploughmarks and seabed scouring were encountered in the area (Games, 2001). At deeper levels (Jurassic/Cretaceous, at thousands of metres depth), hydrocarbons have been discovered and flowed on test (Croker and Shannon, 1987).

Within this dynamic setting, a unique and intriguing benthic ecosystem was rediscovered some 10 years ago (Hovland et al., 1994). Deep-sea, cold-water coral species such as *Lophelia pertusa* (L.) and *Madrepora oculata* (L.), together with their associated fauna and in conjunction with the currents and sedimentation processes, have created giant mound structures (up to 200 m above the seabed and 1500 m across) in three areas in the Porcupine Basin (the 'Belgica', 'Hovland' and 'Magellan' provinces, Fig. 1). De Mol et al. (2002) identified these structures as 'coral banks': mound-like, topographic elevations on the seafloor, consisting partly or completely of corals.

The occurrence of the corals in the Porcupine Basin was first reported more than a century ago (Thomson, 1873), and Le Danois (1948) discussed the presence of 'massifs corralliens' on the Porcupine slopes in 1948. However, it was not until 1994 that the first publication appeared in which the mounds were imaged and described on seismic profiles (Hovland et al., 1994). And still the origin and formation mechanisms of the structures are not completely understood. They have been linked to the presence of strong currents and to sedimentation processes in the area (Kenyon et al., 1998; De Mol et al., 2002), but also to the presence of hydrocarbons and the leakage of shallow gas (Hovland et al., 1994; Henriet et al., 1998), or to a combination of all of these.

The mounds of the Porcupine Basin have been studied by means of several techniques, amongst which are high-resolution and industrial seismics, multibeam echosounding, sidescan sonar surveys, shallow cores and seabed video recording (e.g. Kenyon et al., 1998). This paper focuses on the first interpretation of an industrial 3D seismic data set covering part of the Magellan mound province (containing mainly buried mounds), interpreted in conjunction with high-resolution 2D seismic data acquired by the RCMG (Renard Centre of Marine Geology, Gent, Belgium) (Fig. 1).

The buried mounds were first discovered on industrial 2D site survey seismic data, obtained in 1996 by the MV *Svitzer Magellan* (Britsurvey, 1997). In 1997, 1998 and 1999, they appeared on the RCMG high-resolution 2D seismics as a dense province of complex, multiple or so-called 'twin' structures (Henriet et al., 1998). In general, the structures were acoustically transparent, occurred at a water depth of c. 600 m and were covered with some 50 m of sediments. Comparison with other mound structures in the Porcupine Basin allowed their identification as deepwater mounds or coral banks as well. A remarkably large number of mounds were identified within the limited extent of the 2D seismic surveys. Britsurvey (1997) for example counted 80 structures in a site survey of approximately 8 by 9 km. Hence questions arose as to the true 3D morphologies and spatial distribution of these mounds.

This paper therefore aims at illustrating and describing the morphologies and spatial distribution of the buried mounds in the Magellan province, as far as it can be interpreted from the industrial 3D seismic data. Based on this description, the Magellan mounds will be compared to other mounds in the Porcupine Basin and along continental margins, and some hints can be given towards their origin, growth and formation controls.

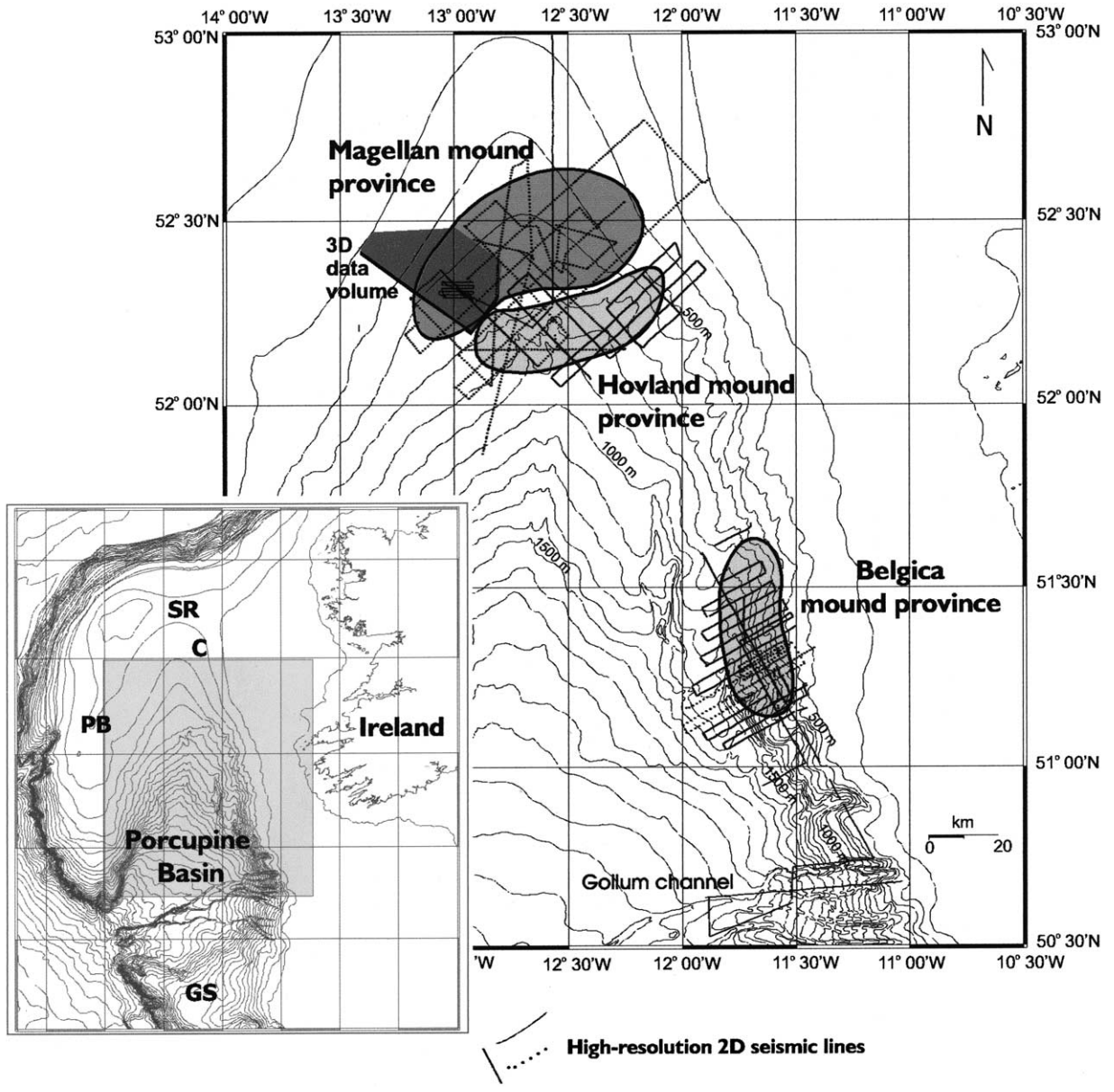

Fig. 1. Location map of the study area, indicating the different mound provinces in the Porcupine Basin. The positions of the high-resolution 1997–1999 2D and the 1998 3D seismic data sets are marked. PB: Porcupine Bank, SR: Slyne Ridge, GS: Goban Spur, C: Connemara Field.

2. Data

This study is based on the upper 400 ms TWT (two-way travel time) of an industrial 3D seismic data volume, recorded in 1998, and provided by Statoil Exploration (Ireland) Ltd and its partners. The data volume covers an area of 1040 km^2 and was sampled at an interval of 4 ms. The original bin size was 12.5 by 12.5 m but was averaged later on in this study to 25 by 25 m to obtain easier data handling. Processing was performed by Western Geophysical, and included (in addition

to various filters and amplitude restorations) the implementation of deconvolution, dip move-out and migration of the data. The final product was presented as a zero-phase data volume in UTM coordinates (zone 28N, datum ED50, ellipsoid international 1924).

The 400 ms TWT of data obtained represents a section of the geological sequence which is sufficiently deep to contain the mound structures plus an underlying sequence with chaotic facies. Both types of features were recognised on the high-resolution 2D seismics as well, and the present interpretation is based on both sets of information. In plan view, however, the 3D seismic data volume does not cover the full spatial extent of the buried mound phenomenon ('Magellan province', Fig. 1). Results of the 2D seismic surveys carried out by the RCMG have shown that a large part of the mound province is situated to the northeast of the 3D seismic volume. Still, with its extent of 1040 km^2, a fairly large and representative portion of the province could be studied in a detailed way (Fig. 1).

The high-resolution 2D seismic data used to refine the 3D interpretations were acquired by the RCMG during its cruises in the Porcupine Seabight in 1997, 1998 and 1999 on board of the RV *Belgica* (Fig. 1). Both sparker (500 J) and watergun (140 bar) sources were used, along with a single-channel surface streamer. The vertical resolution of the data is about 1 ms TWT (~75 cm), the horizontal resolution is c. 45 m, and the profiles contain c. 350 ms TWT of useful data.

3. Automated mapping of mounds and moats

3.1. Methods

3.1.1. Mapping of key reflections

A first step in the analysis was the picking and mapping of 'key reflections' in the 3D volume. They are depicted in Fig. 2. The key reflections were chosen based on the integrated seismic data set (both 2D and 3D data), for the visualisation of the morphology of the sedimentary sequences.

The '**top slide unconformity**' (TS unconformity),

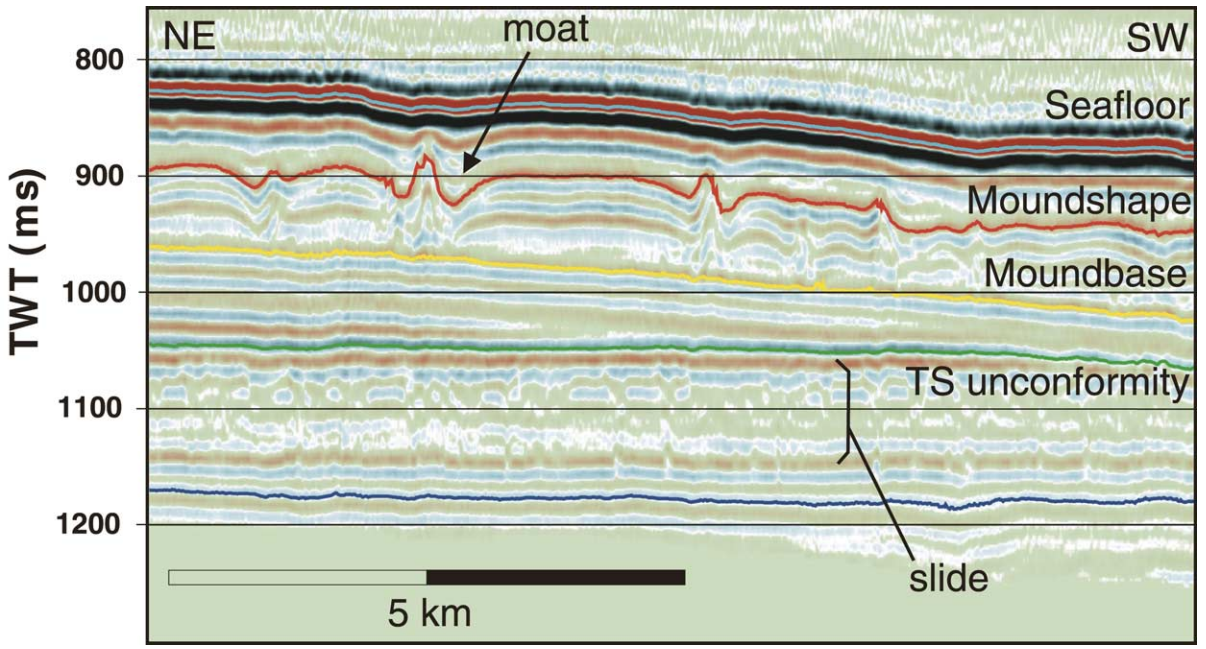

Fig. 2. Representative profile from the 3D seismic data set, showing the key reflections used in this study. The position of the profile is indicated on the map in Fig. 4.

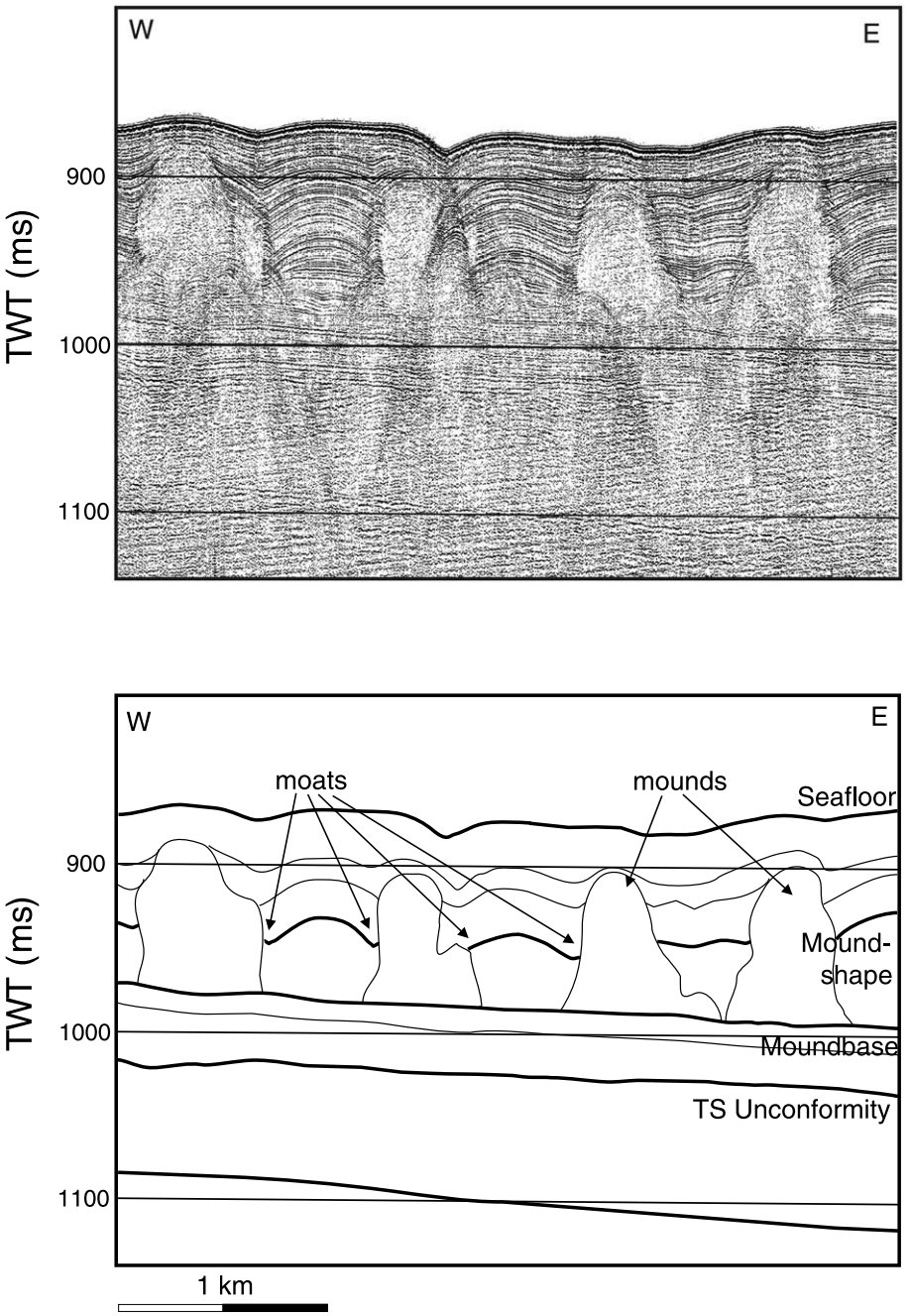

Fig. 3. High-resolution 2D seismic profile across the Magellan mound province. The position of the profile is indicated on the map in Fig. 4. The key reflections mapped from the 3D seismic volume are shown on the lower section. Mounds appear as acoustically transparent zones between the seabed and the moundbase reflection. The depressions in the reflections adjacent to the mounds are interpreted as moats, caused by current scouring of the seabed around the giant structures. Notice the lack of acoustic blanking under the mounds: apart from diffraction effects, reflections are continuous and without reduction of amplitude.

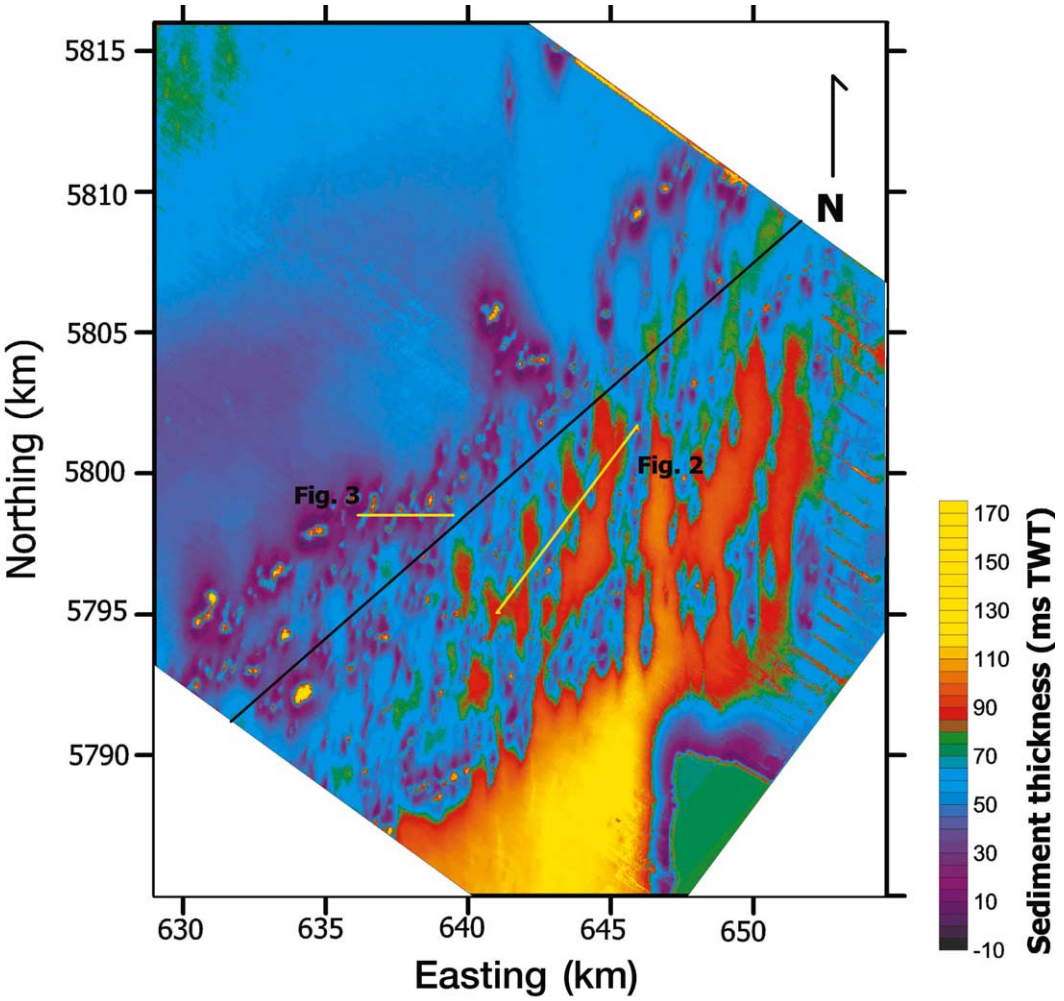

Fig. 4. MB–MS isopach map, indicating the location of the representative profiles shown in Figs. 2 and 3 and the NE–SW divide used for estimation of spatial variability in mound properties (thickness indicated in ms TWT). Mounds appear as positive anomalies, while moats represent zones with lower values in sediment thickness.

a sharp unconformity defined by the onlapping and downlapping of above-lying reflections, delimits the sedimentary sequences before and after a major change in sedimentation pattern. It forms the top of a chaotic facies, interpreted as a major 'slab slide' with a limited downslope movement (Huvenne et al., 2002).

The choice for the '**moundbase**' (MB) reflection became obvious after the initial inspection of the data. Mounds could be recognised as small, sometimes conical zones with irregular reflections, corresponding to the acoustically blanked zones on the 2D seismic data (Fig. 3; Henriet et al., 1998). They all appeared to be seated on the same reflection, which was picked and mapped.

The '**moundshape**' (MS) reflection was chosen to demonstrate the shapes of mounds and 'moats' (the depressions in the reflections adjacent to the mounds). It marks the upper boundary of a seismic facies containing parallel reflections, dipping towards the mounds. In the 3D seismic data, it is also the first reflection that can be traced over the mounds (other reflections below become chaotic and non-continuous in the mounds). Above this

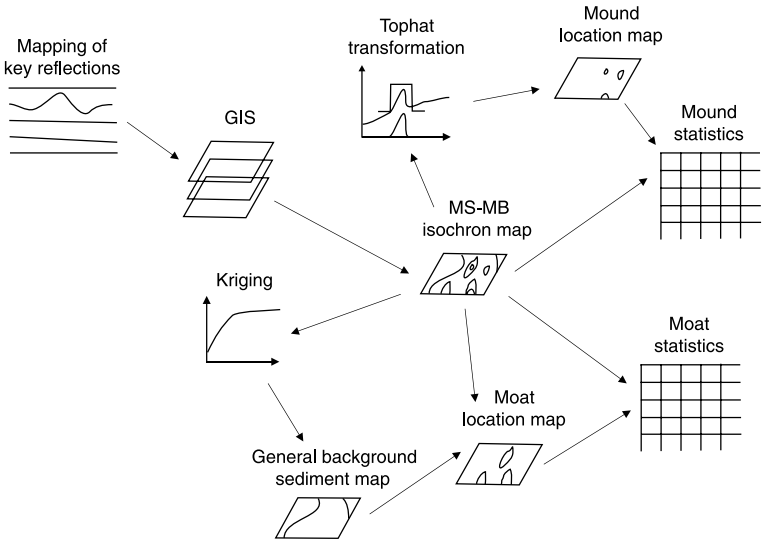

Fig. 5. Flowchart summarising schematically the different steps in the (semi-)automatic extraction method of mound and moat measures.

MS reflection, the moats gradually become less prominent and infilled, while the mounds gradually become buried. Hence, the moundshape reflection is interpreted as the surface at which the mounds and moats had their strongest expression at the seafloor.

Finally, the '**seafloor**' was picked as a distinct feature and kind of 'reference plane'.

3.1.2. *Automated mapping of mounds and moats*

As the main aim of this investigation was the spatial and morphological study of the mounds, the analysis was undertaken within a GIS (Geographical Information System with as key software: Idrisi (Clark Laboratories) and Surfer (Golden Software)). The analysis was based on the time-structure maps (or 'images') of the picked MB and MS reflections and the TS unconformity, and the isopach map of the sediment thickness between MB and MS.

The MB–MS isopach map (Fig. 4) gives the best representation of the mounds and their setting (at the moment of deposition of MS), as the thickness at the mound locations represents the mound height above the common moundbase, and their spatial distribution is well illustrated. In this image, mounds were defined as sharp positive anomalies compared to the surrounding values (background sediment), while moats form negative anomalies. The algorithms for their mapping were based on this principle. However, different algorithms had to be used for the mapping of both features, as there was a difference in characteristics. The slopes of the mounds have much higher gradients, and the mounds are much smaller in cross-sectional area than the moats. The full GIS procedure is presented schematically in Fig. 5.

First, a 'general background sediment thickness', map was estimated, as if there had not been any mounds in the area. Therefore 250 points were chosen according to a stratified random scheme, and the sediment thickness values at these locations on the MS–MB isopach map were used as input data set for an interpolation using ordinary kriging (Davis, 1986; Chilès and Delfiner, 1999). These 250 points also included the occasional samples on mounds and in moats, but these were considered part of the natural variability. The interpolated/estimated result was subtracted from the original isopach map. Negative values in this image represented moat areas, but the algorithm failed to separate the mounds correctly.

Hence, a range of other possible techniques were tried out for the automated mapping of the mounds. The technique which appeared to give

the best results was the application of a tophat transformation, an algorithm known from mathematical morphology (Serra, 1982). It is normally used to remove speckle in radar or satellite images, but can also be used for example to localise galaxies and stars in high-resolution images of the sky (Jandir Candeas et al., 1997). The algorithm can separate positive (or negative) peaks from their local background, independent of the general spatial trend in the image (Serra, 1982). It is based on the use of a 'structuring element', comparable to the moving window or 'kernel' used in filters (Young et al., 1995). In this case the simplest possible structuring element was used, being a square of 11×11 pixels, which appeared to be the appropriate size to capture the mounds in the image.

3.2. Mapping results

Using the tophat transformation algorithm, a total of 327 'structures' were found in the data set (Fig. 6). Manual inspection showed that 6.4% were artefacts, while some 7% of the actual

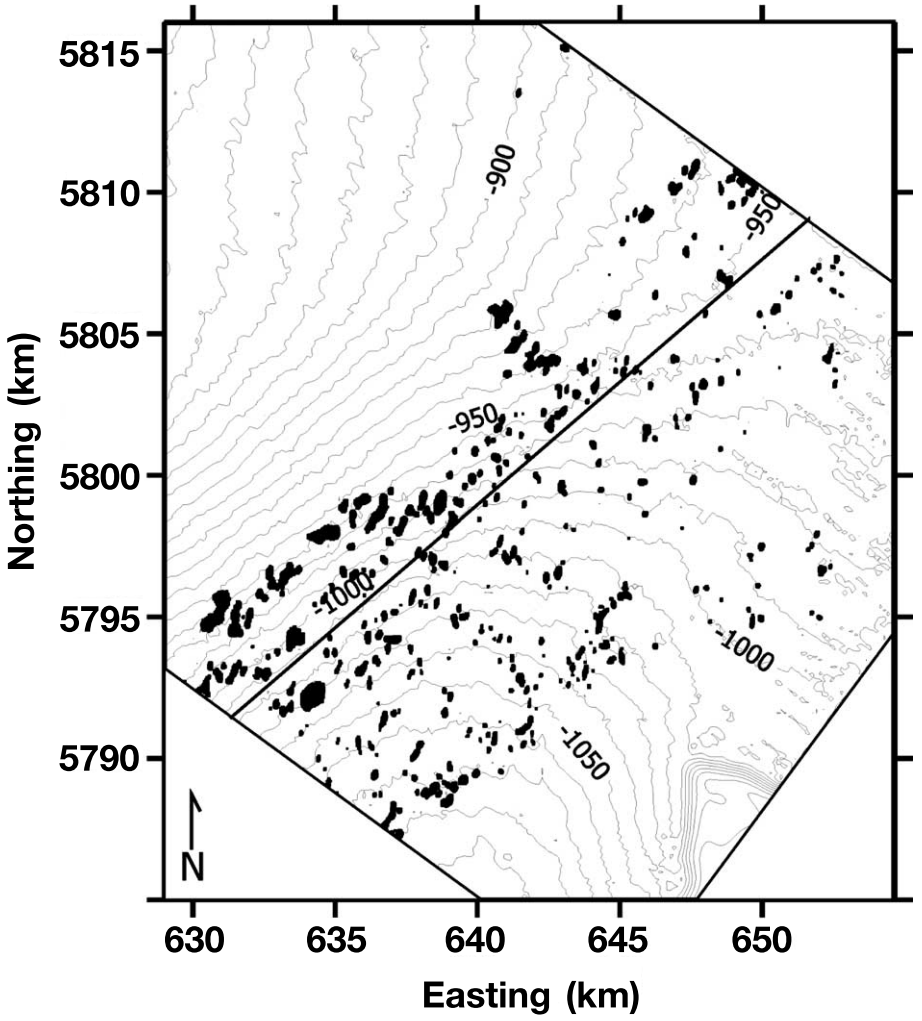

Fig. 6. Time-structure map of the moundbase reflection. Contours are in ms TWT, with an interval of 10 ms. Mound locations and shapes, as mapped from the tophat transformation, are plotted on top (black irregular dots). Although the mounds seem to be restricted below the 920-ms TWT contour, there is no obvious relationship between the two sets of information.

mounds were overlooked by the algorithm (mainly smaller ones, nearly buried already at the MS level). Nevertheless, these were very good results when compared to the other algorithms tested. The map gives a good overview of the mound pattern and gives an idea of the variability in size and shape.

After manual removal of the artefacts, 306 mounds were used for further statistical analysis. However, it has to be kept in mind in the subsequent interpretations that the results picture the situation at the moment of deposition of the MS horizon. Although this appears to be the level at which the mounds generally were expressed the strongest on the seafloor, some very small mounds had already been buried by that time, and the general pattern might have been slightly different at other moments in time.

The mapping of the moats resulted in 172 structures, pictured in Fig. 7. In this case the algorithm did not pick artefacts, although it overlooked some 7% of the moats, all small and shallow structures. The moats appear on the map as structures elongated in a N–S direction. Quite often the moats of several mounds are linked into one big structure with irregular (but still elongated)

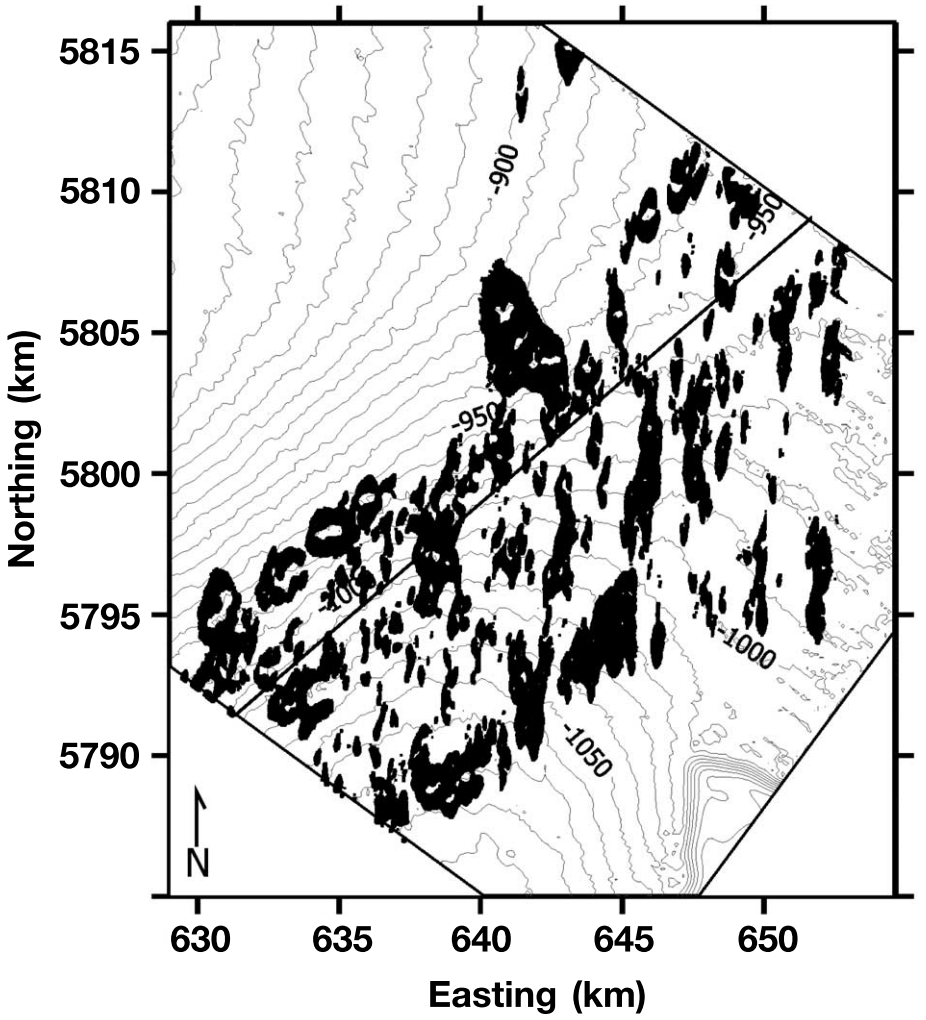

Fig. 7. Results of automated mapping of the moats, indicated as dark irregular patches. The contour map in the background is the same as presented in Fig. 6 and shows the depth of the moundbase reflection in ms TWT.

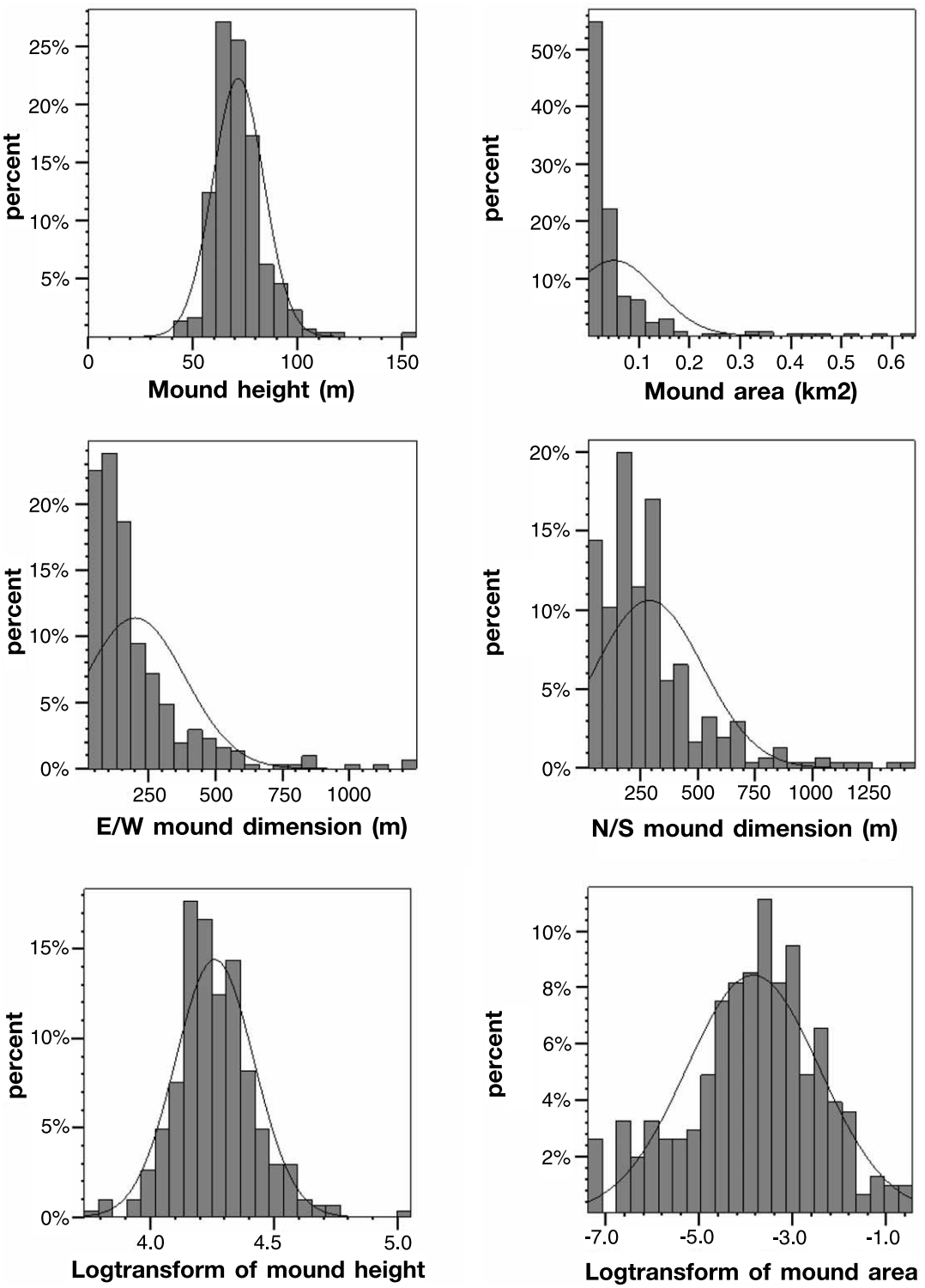
percent
25%
20%
15%
10%
5%
0
50
100
150
Mound height (m)
percent
50%
40%
30%
20%
10%
0.1
0.2
0.3
0.4
0.5
0.6
Mound area (km2)
percent
20%
15%
10%
5%
0%
250
500
750
1000
E/W mound dimension (m)
percent
20%
15%
10%
5%
0%
250
500
750
1000
1250
N/S mound dimension (m)
percent
15%
10%
5%
0%
4.0
4.5
5.0
Logtransform of mound height
percent
10%
8%
6%
4%
2%
-7.0
-5.0
-3.0
-1.0
Logtransform of mound area

Table 1
Descriptive statistics of the mapped mounds

	Height (m)	Area (km^2)	E–W dimension (m)	N–S dimension (m)
Mean	71.7	0.051	201	290
S.D.	12.2	0.085	187	233
Min.	42.9	0.0006	25	25
Max.	156.7	0.645	1250	1449
Skewness	1.70	4.02	2.72	1.94
KS sign.[a]	0.028	0.000	0.000	0.000
KS sign.[a] log-transformed	0.331	0.180	0.010	0.006
t-statistic (paired *t*-test)			−12.781	
Probability for equality of means			0.000	

[a] KS sign.: significance result of the Kolmogorov–Smirnov test for normality.

shape. These structures were counted as one in the subsequent analyses.

4. Mounds, moats, and their spatial distribution

4.1. Methods

The mapping results (Figs. 6 and 7) were used as templates to extract information on the mound and moat morphology from the original MS–MB isopach map. Within the GIS the height of the mounds (from the MB reflection) and the depth of the moats, their cross-sectional area (at the MS level), and their length in N–S and E–W directions were extracted automatically. The heights and depths were measured in ms TWT, and converted to metres, using an average sound velocity in the sediments of 1800 m/s (average value for mud and sands with medium compaction, Sheriff and Geldart, 1995). Because there are no clear pull-ups or pull-downs under the mounds in the seismic data (both 3D and 2D), it is assumed that the mounds and surrounding sediments have largely comparable sound velocities.

For both mounds and moats, the correlation coefficients between the different feature characteristics were calculated, and the means of the N–S and E–W dimensions of both types of structures were compared using a two-sided, paired *t*-test (Davis, 1986).

4.2. Statistical results

4.2.1. Descriptive mound statistics

Mounds occur in a variety of sizes, with shapes varying from single, conical mounds to elongated or complex, multiple shapes (Figs. 4 and 6). The frequency distributions of the different parameters sampled are presented in histograms in Fig. 8, their mean values and standard deviations are summarised in Table 1. The mean height of the Magellan mounds, at the MS level, is some 72 m, while the tallest structures are up to 157 m high. The tallest mounds occur mainly on the western edge of the cluster, and some even reach the seafloor. The mounds are on average 250 m wide, while the mean area is estimated as 0.051 km^2.

All characteristics have a skewed distribution, the area parameter being the most extreme. Kolmogorov–Smirnov tests for normality (Davis, 1986) confirm that the characteristics are not normally distributed (Table 1). However, after logarithmic transformation, a normal distribution is achieved for the height and area characteristics (on a 5% significance limit). The log-normal distribution suggests that mound growth is a natural phenomenon containing some form of pyramidal

Fig. 8. Histograms (frequency distributions) of the mound properties. Curves representing a normal distribution with the same mean and standard deviation as the data are plotted as thin black lines. The two bottom graphs illustrate that after natural logarithmic transformation of the data, the distributions are closer to the normal curve (especially the 'area' parameter).

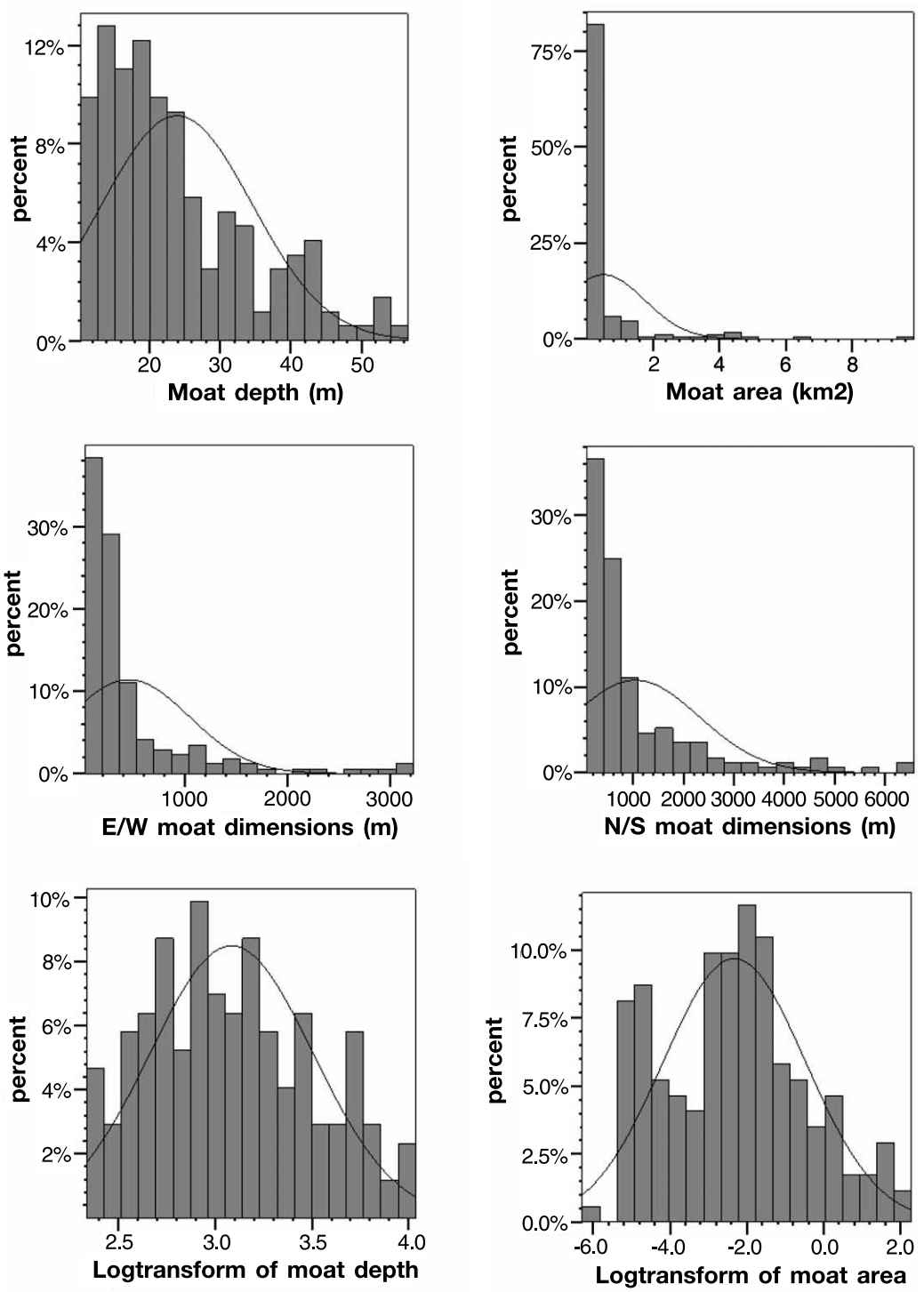

Fig. 9. Histograms of the moat properties. Curves representing a normal distribution with the same mean and standard deviation as the data are plotted as thin black lines. The two bottom graphs illustrate the frequency distribution after natural logarithmic transformation of the depth and area parameter.

Table 2
Pearson correlation coefficients between the different mound characteristics

	Height (m)	Area (km^2)	E–W dimension (m)	N–S dimension (m)
Height (m)	1	0.682	0.641	0.583
Area (km^2)		1	0.928	0.865
E–W dimension (m)			1	0.855
N–S dimension (m)				1

ordering (many small items, few large ones). The distribution, on the other hand, can also be interpreted as an artefact resulting from the sampling resolution. Especially in the horizontally measured values, the smallest items could be smaller than the pixel size (25 m), and hence be discarded from the analysis. However, 2D profiles confirm that no structures smaller than 25 m were present that reached considerable height. The resolution in the vertical direction is better, hence the effect would not be a problem for the height parameter.

The correlation coefficients between the mound characteristics are presented in Table 2. All measures are significantly positively correlated, but the values are especially high for the area parameter, the N–S and the E–W dimensions. Height is not so closely linked to the others, suggesting that the actual vertical growth of the mounds is not directly linked to their width. This will be confirmed by the results of the spatial variability analysis.

The results of the two-sided paired *t*-test indicate that the means of the N–S and E–W dimensions of the mounds are significantly different at the 5% level. Hence mounds are significantly elongated in a N–S direction. This result is supported by the slightly higher correlation coefficient between the E–W dimension and the area, compared to the coefficient between the N–S dimension and the area: it seems to be mainly the E–W dimension that determines the actual cross-sectional area of the mound. Structures with a large N–S dimension can be narrow and elongated, and therefore still have a moderately low area value.

4.2.2. Descriptive moat statistics

The frequency distributions and descriptive statistics of the moat characteristics are presented in Fig. 9 and Table 3. The average moat depth is some 24 m, a little more than one-third of the average mound height between the MB and MS horizons. A high standard deviation, however, indicates a high variability in moat depths over the mapped area. The area of the individual moats is on average an order of magnitude larger than that of the mounds, partly due to the fact that some of them have blended into large 'moat fields'.

The frequency distribution curves of the moat

Table 3
Descriptive statistics of the mapped moats

	Depth (m)	Area (km^2)	E–W dimension (m)	N–S dimension (m)
Mean	23.9	0.51	450	1040
S.D.	10.6	1.24	590	1270
Min.	10.4	0.002	25	75
Max.	56.5	9.85	3220	6570
Skewness	1.00	4.36	2.82	2.25
KS sign.[a]	0.007	0.000	0.000	0.000
KS sign.[a] log-transformed	0.590	0.647	0.121	0.226
t-statistic (paired *t*-test)			−9.239	
Probability for equality of means			0.000	

[a] KS sign.: significance result of the Kolmogorov–Smirnov test for normality.

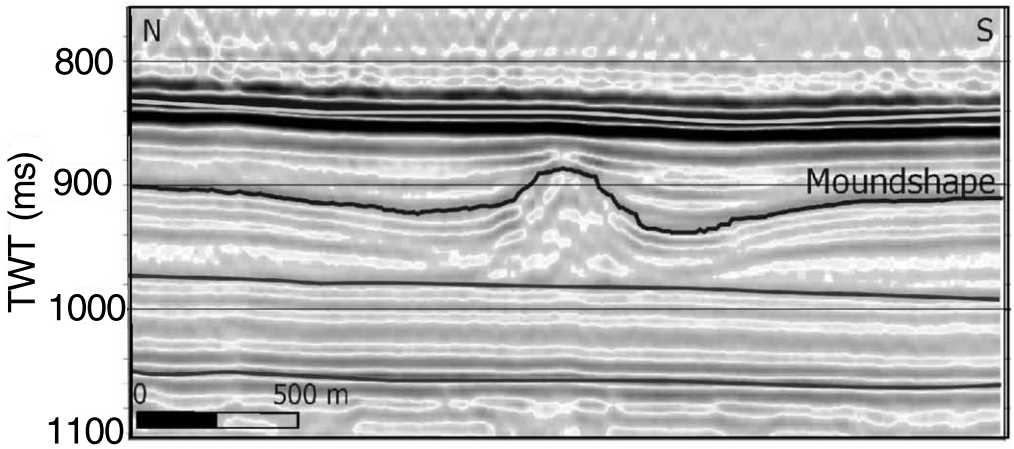
N
S
800
900
1000
1100
TWT (ms)
Moundshape
0
500 m

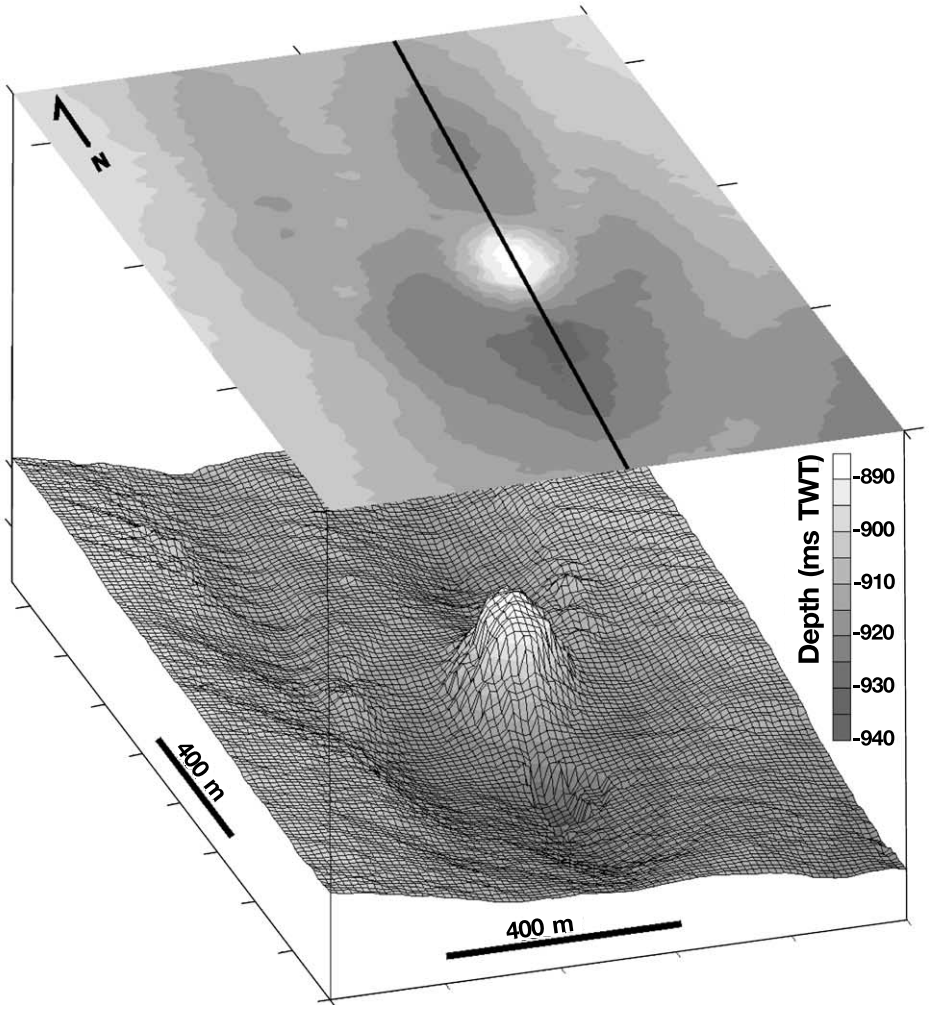
N
Depth (ms TWT)
-890
-900
-910
-920
-930
-940
400 m
400 m

Table 4
Pearson correlation coefficients between the different moat characteristics

	Depth (m)	Area (km^2)	E–W dimension (m)	N–S dimension (m)
Depth (m)	1	0.650	0.740	0.799
Area (km^2)		1	0.907	0.858
E–W dimension (m)			1	0.834
N–S dimension (m)				1

characteristics are similar to those of the mounds: all characteristics are also log-normally distributed. The area, N–S and E–W dimensions of the moats are strongly correlated (Table 4), and the two-sided paired *t*-test indicates that the means of the N–S and E–W dimensions are significantly different at a 5% level. Hence both mounds and moats are elongated in the N–S direction, but the effect is stronger for the moats (ratio of 2.30) than for the mounds (ratio of 1.44). This suggests a strong N–S-directed influence during mound growth and associated moat formation as also shown in Fig. 10.

4.2.3. *Spatial distribution of mounds and mound characteristics*

From the description of the individual mounds, the focus is now shifted to the organisation and structure of the whole group of mounds found in the 3D seismic data set. As mentioned above, 327 structures could be discriminated, concentrated in an area of approximately 350 km^2 in the ESE part of the 3D data set. Hence the mound density in this part of the Magellan province, at the level of the MS reflection, is close to $1/km^2$ (compare with the average mound cross-sectional area of 0.051 km^2). The mound density was also compared northwest and southeast of an arbitrary NE–SW-oriented divide (indicated on Fig. 4). The results (0.91 and 1.06 mounds/km^2) are not seriously different from the overall value (0.93/km^2), which implies that mound density in the Magellan province is generally spatially continuous.

In addition to the mound density, the other mound characteristics may also be prone to local variation. From the seismic profiles and the mound map (Fig. 6) it appears as if the mounds in the east-southeastern part of the cluster are smaller and less complex than the mounds in the west-northwest. Therefore mound and moat characteristics were recalculated northwest and southeast of the arbitrary line mentioned above (Fig. 4), and the means were compared using two-sided *t*-tests (Davis, 1986). Significant differences were found in the horizontal mound dimensions (area, dimension in N–S and E–W direction, Table 5), but the mean heights are essentially equal in both subclusters and in the full data set (71.7 m). In the WNW zone, the average horizontal dimensions of the mounds are larger than in the ESE zone, but the standard deviations are higher there as well. Hence mounds are not only wider there, but there is also a greater variability in mound size and morphology.

The comparison of moat characteristics east and west of the divide shows no statistically significant differences (at the 5% level), although the moat areas and E–W dimensions in the WNW part of the cluster on average are bigger than in the ESE part (Table 6). Depths and N–S dimensions of the moats do not differ very much over the study area. Moats in the ESE part hence seem more elongated than in the WNW part, although they are of similar depth.

Finally the GIS was used to compare the mound locations with the underlying geology

Fig. 10. 3D representation of a small Magellan mound as it appears at the MS reflection. Notice the elongated moat which is deepest at the northern and southern sides of the mound. Both mound and moat are buried by sediments: at the present-day seafloor there is nearly no trace left of the buried structures.

Table 5
Comparison between mound characteristics of the eastern and western parts of the mound cluster

N(w): 107, N(e): 199	Height (m)		Area (km^2)		E–W dimension (m)		N–S dimension (m)	
	W	E	W	E	W	E	W	E
Mean	71.7	71.7	0.085	0.032	280	159	390	237
S.D.	14.2	11.1	0.118	0.051	250	123	290	175
Min.	42.9	50.8	0.0006	0.0006	25	25	25	25
Max.	116.1	156.7	0.645	0.588	1250	825	1450	1099
t-statistic	0.0026		5.4254		5.5948		5.6902	
Probability for equality of means	0.9979		<0.0001		<0.0001		<0.0001	

(within the 3D seismic data volume). Time-structure and isopach maps of all picked horizons were studied, together with maps of shallow faults. No obvious relation between the mound pattern and any of the maps was found.

5. Discussion

The previous sections demonstrated how the industrial 3D seismics, supplemented by 2D high-resolution seismic data, give insight into the structure of the Magellan mound province. Seismic profiles showed that all mounds in the area are seated on one single reflection. The mapping of this and other key reflections revealed mounds of varying size and complexity, generally elongated in a N–S direction and surrounded by even more elongated moats. The dense cluster of mounds, mapped automatically, has a constant average mound height, but spatially varying horizontal mound dimensions.

5.1. Mound morphology

The general mound morphology is described by the statistical results presented in Section 4. The log-normal distribution of the mound characteristics shows that the mound population exhibits a natural 'pyramidal' order with a large number of small mounds and a limited number of large structures. This type of distribution is often encountered in geology (Davis, 1986).

The seismic profiles (especially the high-resolution 2D profiles) show that at the MB level, several small structures and irregularities are present. They can be interpreted as very small coral build-ups, indicating that the initial coral growth and start-up of the mound development must have been spatially extensive. Later on, a limited number of mounds survived from this massive start-up pool, and these developed further to form the large structures mapped from the 3D seismics. Therefore, the largest mounds appear to have started growing from a broad base or large coral

Table 6
Comparison between moat characteristics of the eastern and western parts of the mound cluster

N(w): 56, N(e): 116	Depth (m)		Area (km^2)		E–W dimension (m)		N–S dimension (m)	
	W	E	W	E	W	E	W	E
Mean	24.7	23.6	0.63	0.45	570	390	1100	1020
S.D.	11.4	10.3	1.55	1.06	710	520	1260	1270
Min.	10.4	11.0	0.006	0.002	75	25	75	75
Max.	53.5	56.5	9.85	6.33	3220	2950	6520	6570
t-statistic	0.6186		1.9207		1.8723		0.4071	
Probability for equality of means	0.537		0.0564		0.0629		0.6845	

patch rather than having grown much wider during the course of time. Ring-shaped reefs as described from 2D seismic data by Henriet et al. (1998), however, were not encountered in the 3D seismic volume. Most probably the 'twin' structures, as mentioned by these authors, resulted from the imaging on 2D seismic profiles of closely spaced Magellan mounds.

5.2. Comparison with other mound occurrences

Compared to the mounds in the other Porcupine provinces (Fig. 1), the Magellan structures are, on average, the smallest. De Mol et al. (2002) reported average mound heights (measured from base to top on seismic profiles) of some 100 m and maxima of up to 250 m in the Hovland province, and 70–200 m in the Belgica province. Hovland mounds can be up to 5 km in length and 1.5 km in width, while Belgica mounds reach up to 1.5 km across. Mound densities can be estimated as 1 mound per 10 km^2 (38 mounds), and 1 mound per 7 km^2 (63 mounds) in each province respectively. In comparison, the Magellan mounds are much more numerous, and have a much higher spatial density.

Mound structures comparable to those in the Porcupine Basin are found at other locations as well. The structures most similar to the Porcupine mounds were reported from the Rockall Trough Margins (van Weering et al., 2003), where they can reach heights of 300 m and can have an extremely complex morphology and structure. Along the Florida–Hatteras slope partly cemented lithoherms/coral banks were found, capped with deep-water corals (e.g. Paull et al., 2000). They have a size similar to that of the Magellan mounds and their spatial density reaches 1 mound per 3 km^2, which is slightly lower than found in this study. Hovland et al. (1998) and Mortensen (2000) reported ahermatypic coral (*Lophelia*) banks off mid-Norway with a local density of up to 1.2 mounds per km^2. These structures occur at water depths of some 300 m, are slightly smaller than the Magellan mounds (reach up to 31 m above the seabed), but are much less numerous (some 57 mounds were described in total). Although this list does not give a full review of all possible mounds and cold-water coral (*Lophelia*) banks in the world's oceans (for a full review on cold-water corals in the Atlantic, see Rogers, 1999), it illustrates the unique position of the Magellan mounds, which are extremely numerous and densely spaced.

5.3. A sudden start

Since all mounds are rooted on the same reflection, they all started growing at one moment in time (within the time resolution of the seismics). A similar pattern has been found in the other mound provinces in the Porcupine Basin where both the Belgica and Hovland mounds had one start-up phase (De Mol et al., 2002). The Rockall mounds show at least two and probably even more pulses of mound formation or renewed mound expansion and growth; however, all above a clear reflector named 'C10', dated as of Early Pliocene age (Stoker et al., 2001; van Weering et al., 2003). McDonnell (2001), based on seismic facies correlation between the Rockall and Porcupine basins and on the extrapolation of well datings in the Porcupine, interprets the MB reflection in the Magellan province and the base of the mounds in the Hovland and Belgica provinces to be equal to this 'C10' reflector too. Hence mound initiation would have taken place in the Porcupine Basin in the Early Pliocene. Britsurvey (1997), however, indicates a 'near base Quaternary' age for the MB reflection (based on correlation with nearby surveys and wells), and thus a Late Pliocene, Early Pleistocene age for the mound initiation in the Magellan province. De Mol et al. (2000) used the extrapolation of sedimentation rates obtained from a shallow core in the Hovland area to interpret the MB reflection as of Late Pliocene age too. De Mol et al. (2002) also doubt the simultaneous initiation of all mound growth in the Porcupine Basin, and suggest that the Belgica mounds could be slightly older than the Hovland and Magellan mounds. A regional Late Pliocene hiatus in the geological sequence from the Rockall Trough to the Goban Spur was reported by Pearson and Jenkins (1986). De Mol et al. (2002) relate this to the reintroduction of the Mediterranean Outflow Water in

the NE Atlantic after the Late Miocene–Early Pliocene Messinian salinity crisis in the Mediterranean Sea. This event will have affected the chemical and physical water conditions in the Porcupine Seabight and might have introduced larvae of *Lophelia* and associated coral species, as the oldest fossil records of the species are reported from the Mediterranean Sea.

5.4. Spatial setting

The map of the mound locations (Fig. 6) shows that the occurrence of the Magellan mounds is, not only in time, but also in space, a sharply confined event. A few different hypotheses have been put forward to explain the spatial occurrence of deepwater corals, mounds and mound provinces. Hovland et al. (1994) and Hovland and Thomson (1997) linked the occurrence of the mounds to hydrocarbon seepage along faults. Henriet et al. (1998) suggested a glacially influenced destabilisation of gas hydrates, possibly linked to large submarine landslides. Frederiksen et al. (1992), Rogers (1999) and Freiwald (2003), on the other hand, stressed the importance of the physico-chemical characteristics of the seawater, the presence and interaction of certain seawater masses and the presence of hard settling grounds for the corals.

The data set used in this study showed no evidence for shallow faults or conduits located specifically under the Magellan mounds. McDonnell (2001) also found no consistent relation between mound occurrences and deeper faults in the Porcupine Basin. The chaotic horizon under the TS unconformity was interpreted as a slab slide (Huvenne et al., 2002), but it underlies only part of the Magellan province as can be seen on 2D seismic profiles east of the 3D data block (see also Britsurvey, 1997). Hence it seems unlikely that the occurrence of this slide has influenced the location of the Magellan mound province. The physical oceanography of the area has clearly influenced the mound growth and seabed morphology from the beginning of the mound development onwards (as shown by the moat formation), hence it is suggested that the oceanographic conditions have largely determined the mound initiation as well. Also De Mol et al. (2000) and McDonnell (2001) suggested climatic controls and bottom currents as probable controls for mound and coral distribution and pattern.

5.5. Spatial variability

The mapping of the Magellan mounds shows that wider and more complex mounds could grow in the WNW part of the cluster, although they still do not reach the size and complexity of the mounds in the other Porcupine provinces (De Mol et al., 2002) or in the Rockall Trough (van Weering et al., 2003). The MS–MB isopach map (Fig. 4) also shows that the general sediment thickness decreases towards the WNW edge of the mound cluster, and beyond. This can be seen on NW–SE-directed profiles too: reflections are onlapping the MB horizon, and are prograding towards the northwest. The gentle depression in the MB reflection seems to have been gradually filled. Hence it seems that the WNW mounds experienced less sedimentation stress than their ESE neighbours, especially in the initial stages. This could have affected the initial expansion of the *Lophelia* colonies, and in this way the width of the mound foundations. It could have been one of the reasons for the larger size and greater complexity of the WNW mounds, the change in environmental conditions creating a spatially changing mound morphology. Besides this, it is also possible that the mounds on the WNW edge took advantage of their position on the outer rim of the province, on the highest positions.

The average mound height, on the other hand, remained remarkably constant over the area (within the time frame of the MS horizon) and seems to be less influenced by the sedimentation stresses. It probably reflects an inherent vertical growth capacity of the faunal associations building the coral banks. Still, only on the western edge of the mound cluster was the sedimentation low enough to allow a few mounds to reach the present-day seabed.

5.6. Moats and currents

As mounds slowly grew, and slowly became

embedded in the surrounding sedimentary sequences, moats developed around them. The pinching out of the sediments towards the mounds indicates a locally limited deposition, non-deposition or, in some locations, maybe even erosion. Similar 'dips' have been reported from other mound structures (e.g. the Rockall Mounds, van Weering et al., 2003). They are attributed to scouring by currents. In the Magellan province, the current effects are strong, shaping the scour marks into elongated moats. However, scour marks or obstacle marks are generally described as crescent-shaped at the upstream side of the obstacle, and containing a long depositional tail or a tail depression at the downstream side (Karcz, 1968; Werner et al., 1980). The mounds in the Magellan province do not have a depositional tail, are elongated in a N–S direction and in general have elongated scoured depressions at both the northern and southern sides of the mounds. This indicates a N–S-directed, reversing current (Werner et al., 1980), and is comparable to e.g. tidal scour around bridge piers (Stumm et al., 2000) or the scour marks found around shipwrecks in strongly tidally influenced seas (Moerkerke, personal communication). In these conditions the average residual current is small, while the tidal flows are much more important. The moats in the Magellan province indicate that a N–S-directed, reversing current was present for a long time. It is possible that this current had a tidal frequency, because present-day current measurements in the area indicate that the residual current is fairly weak (1–5 cm/s; White, 2001), while tidal effects are considerable (M2 tide of 5–10 cm/s in the slope region west of Ireland, with an extra intensification of the diurnal tide in the northern end of the Porcupine Seabight). Because most moats can be traced in the sedimentary sequences from nearly the moundbase up to the seabed (staying parallel to themselves), it is reasonable to assume that the present-day tidal influence is comparable to the situation during mound development. The conditions may be a little less extreme at present, however, as moats have partially filled since the deposition of the MS reflection, and currents may have been stronger at that time. To what extent these tidal current signals were due to internal tides rather than barotropic tides is not clear yet. Internal waves and tides are periodic oscillations in the water column, formed when vertically stratified waters are forced over an irregular bottom topography, e.g. the shelf edge (Huthnance, 1989). As internal tides and waves are mentioned at several locations in the Porcupine Seabight (e.g. Rice et al., 1990), and their possible influence on *Lophelia* corals and coral banks has also been discussed (e.g. Frederiksen et al., 1992), it would be worthwhile to estimate their role in the Magellan province.

The fact that the moats in the southeastern part, although not statistically significantly, seem to be a little smaller and more elongated than in the northwestern part of the cluster can be interpreted together with the spatial variation in mound size. Smaller mound structures will have induced narrower scour marks.

6. Conclusions

This paper presents the first results of a spatial and morphological study of the Magellan mounds in the Porcupine Basin. The study was based on an industrial 3D seismic volume, complemented by high-resolution 2D seismic data. Mapping and GIS tools were used, together with image analysis techniques such as mathematical morphology algorithms (tophat transformation). They allowed the description and statistical analysis of mound morphologies and spatial mound distributions.

Mounds in the Magellan province were – at the time of deposition of the MS horizon – on average 72 m high and 250 m wide. This is smaller than most mounds in the surrounding areas (Porcupine Basin and Rockall Trough), but the Magellan mounds are much more numerous and have a very high spatial density (1 mound/km^2). They represent an important 'volume' of mound growth along the NE Atlantic margin, and are exceptional in terms of their large numbers.

Mound size and spatial density are constant over the zone studied, but the horizontal dimensions of the mounds increase towards the WNW edge of the province. Sedimentation stress seems

to have been less in that direction, allowing more complex and wider mounds to develop, and allowing a few mounds to pierce through the seafloor.

The Magellan mounds are significantly elongated in a N–S direction, and are associated with elongated moats, scoured by currents. The elongation is considered to be related to a reversing current action, possibly of tidal frequency, such as observed on the present-day seabed of the Magellan province.

This data set further shows that mound growth in the Porcupine Basin started as a sudden 'event', sharply confined in time and space. The bottom currents and oceanographic characteristics of the prevailing water masses seem to have played a role in this mound initiation, but the real initiation process is still unclear. Deeper seismic data, drilling results and the integration of other types of data sets (core loggings, video and sidescan images, ROV dives etc.) are currently worked on or are planned for the further investigation of the mound phenomenon.

Acknowledgements

The authors are very grateful to Statoil Exploration (Ireland) Ltd, its partners Conoco (U.K.) Ltd, Enterprise Energy Ireland Ltd and Dana Petroleum plc and Chevron U.K. Ltd for the provision of the 3D seismic data volume. Part of this research was carried out in the framework of the EC Contract 'GEOMOUND' (5th Framework programme) and of the Ghent University project 'Porcupine-Belgica' (BOF). We also wish to thank Pieter Van Rensbergen for the assistance at the start of the 3D study, and David Van Rooij for the 'Porcupine discussions'. V.H. and B.D.M. are PhD students funded through the FWO-Flanders and the IWT respectively.

References

Britsurvey, 1997. Total Oil Marine plc, site survey Irish Block 35/17-1, 14/11/96-13/12/96, final report (report released by Petroleum Affairs Division, Dublin).

Chilès, J.-P., Delfiner, P., 1999. Geostatistics: Modelling Spatial Uncertainty. John Wiley and Sons, Chichester, 695 pp.

Croker, P.F., Shannon, P.M., 1987. The evolution and hydrocarbon prospectivity of the Porcupine Basin, offshore Ireland. In: Brooks, J., Glennie, K.W. (Eds.), Petroleum Geology of North West Europe. Graham and Trotman, London, pp. 633–642.

Davis, J.C., 1986. Statistics and Data Analysis in Geology, 2nd edn. John Wiley and Sons, Chichester, 646 pp.

De Mol, B.S.G., Van Reusel, A., De Berg, B., Henriet, J.-P., 2000. 'Hovland' mounds in Porcupine Seabight, NE Atlantic: biological zonation and environmental control. EOS Trans. AGU F81, 636.

De Mol, B., Van Rensbergen, P., Pillen, S., Van Herreweghe, K., Van Rooij, D., McDonnell, A., Huvenne, V., Ivanov, M., Swennen, R., Henriet, J.-P., 2002. Large deep-water coral banks in the Porcupine Basin, southwest of Ireland. Mar. Geol. 188, 193–231.

Frederiksen, R., Jensen, A., Westerberg, H., 1992. The distribution of the scleractinian coral *Lophelia pertusa* around the Faroe Islands and the relation to internal tidal mixing. Sarsia 77, 157–171.

Freiwald, A., 2003. Reef-forming cold-water corals. In: Wefer, G., Billet, O., Hebbeln, D., Jorgensen, B.B., Schlüter, M., van Weering, T. (Eds.), Ocean Margin Systems. Springer, Heidelberg, pp. 365–385.

Games, K.P., 2001. Evidence of shallow gas above the Connemara oil accumulation, block 26/28, Porcupine Basin. In: Shannon, P.M., Haughton, P.D.W., Corcoran, D.V. (Eds.), The Petroleum Exploration of Ireland's Offshore Basins. Geol. Soc. London Spec. Publ. 188, 361–373.

Henriet, J.-P., De Mol, B., Pillen, S., Vanneste, M., Van Rooij, D., Versteeg, W., Croker, P.F., Shannon, P.M., Unnithan, V., Bouriak, S., Chachkine, P., Porcupine-Belgica 97 Shipboard Party, 1998. Gas hydrate crystals may help build reefs. Nature, 391, 648–649.

Hovland, M., Croker, P.F., Martin, M., 1994. Fault-associated seabed mounds (carbonate knolls?) off western Ireland and northwest Australia. Mar. Pet. Geol. 11, 232–246.

Hovland, M., Mortensen, P.B., Brattegard, T., Strass, P., Rokoengen, K., 1998. Ahermatypic coral banks off Mid-Norway: evidence for a link with seepage of light hydrocarbons. Palaios 13, 189–200.

Hovland, M., Thomson, E., 1997. Cold-water corals – are they hydrocarbon seep related? Mar. Geol. 137, 159–164.

Huthnance, J.M., 1989. Internal tides and waves near the continental shelf edge. Geophys. Astrophys. Fluid Dyn. 48, 81–106.

Huvenne, V.A.I., Croker, P.F., Henriet, J.-P., 2002. A refreshing 3-dimensional view of an ancient sediment collapse and slope failure. Terra Nova 14, 33–40.

Jandir Candeas, A., de Mendonça Braga Neto, U., Costa de Barros Carvalho Filho, E., 1997. A mathematical morphology approach to the star/galaxy characterization problem. J. Braz. Comput. Soc. 3, 263–285.

Karcz, I., 1968. Fluviatile obstacle marks from the wadis of

the Negev (Southern Israel). J. Sediment. Petrol. 38, 1000–1012.

Kenyon, N.H., Belderson, R.H., Stride, A.H., 1978. Channels, canyons, and slump folds on the continental slope between South-West Ireland and Spain. Oceanol. Acta 1, 369–380.

Kenyon, N.H., Ivanov, M.K., Akhmetzhanov, A.M. (Eds.), 1998. Cold water carbonate mounds and sediment transport on the Northeast Atlantic Margin. IOC Technical Series 52, UNESCO, 178 pp.

Le Danois, E., 1948. Les profondeurs de la mer. Payot, Paris, 303 pp.

Moore, J.G., Shannon, P.M., 1991. Slump structures in the Late Tertiary of the Porcupine Basin, offshore Ireland. Mar. Pet. Geol. 8, 184–197.

McDonnell, A., 2001. Comparative Tertiary Basin Development in the Porcupine and Rockall Basins. PhD Thesis, University College, Dublin, 175 pp.

Mortensen, P.B., 2000. *Lophelia pertusa* (Scleractinia) in Norwegian Waters. Distribution, Growth and Associated Fauna. PhD Thesis, University of Bergen, Bergen.

Paull, C.K., Neumann, A.C., am Ende, B.A., Ussler, W., Rodriguez, N.M., 2000. Lithoherms on the Florida-Hatteras slope. Mar. Geol. 166, 83–101.

Pearson, I., Jenkins, D.G., 1986. Unconformities in the Cenozoic of the North-East Atlantic. In: Summerhayes, C.P., Shackleton, N.J. (Eds.). North Atlantic Palaeoceanography. Geol. Soc. Spec. Publ. 21, 79–86.

Pingree, R.D., Le Cann, B., 1989. Celtic and Armorican slope and shelf residual currents. Prog. Oceanogr. 23, 303–338.

Rice, A.L., Thurston, M.H., New, A.L., 1990. Dense aggregations of a hexactinellid sponge, *Pheronema carpenteri*, in the Porcupine Seabight (northeast Atlantic Ocean), and possible causes. Prog. Oceanogr. 24, 179–196.

Rogers, A.D., 1999. The biology of *Lophelia pertusa* (Linnaeus 1758) and other deep-water reef-forming corals and impacts from human activities. Int. Rev. Hydrobiol. 84, 315–406.

Serra, J., 1982. Image Analysis and Mathematical Morphology. Academic Press, London, 610 pp.

Shannon, P.M., 1991. Development of Irish offshore sedimentary basins. J. Geol. Soc. London 148, 181–189.

Sheriff, R.E., Geldart, P., 1995. Exploration Seismology. Cambridge University Press, Cambridge, 592 pp.

Stoker, M.S., van Weering, T.C.E., Svaerdborg, T., 2001. A Mid- to Late Cenozoic tectonostratigraphic framework for the Rockall Trough. In: Shannon, P.M., Haughton, P.D.W., Corcoran, D.V. (Eds.), The Petroleum Exploration of Ireland's Offshore Basins. Geol. Soc. London Spec. Publ. 188, 411–438.

Stumm, F., Chu, A., Reynolds, R.J., 2000. Delineation of tidal scour through marine geophysical techniques at Sloop Channel and Goose Creek Bridges, Jones Beach State Park, Long Island, New York. USGS Water-Resources Investigations Report 00-4033, Coram, NY, 18 pp.

Thomson, C.W., 1873. The Depths of the Sea. MacMillan, London, 527 pp.

Tudhope, A.W., Scoffin, T.P., 1995. Processes of sedimentation in Gollum Channel, Porcupine Seabight: submersible observations and sediment analyses. Trans. R. Soc. Edinburgh Earth Sci. 86, 49–55.

Van Rooij, D., De Mol, B., Huvenne, V., Ivanov, M., Henriet, J.-P., 2003. Seismic evidence of current-controlled sedimentation in the Belgica mound province, upper Porcupine slope, southwest of Ireland. Mar. Geol. 195, 31–53.

van Weering, T.C.E., de Haas, H., de Stigter, H.C., Lykke-Andersen, H., Kouvaev, I., 2003. Structure and development of giant carbonate mounds at the SW and SE Rockall Trough Margins, NE Atlantic Ocean. Mar. Geol. 198, S0025-3227(03)00095-1

Werner, F., Unsöld, G., Koopman, B., Stefanon, A., 1980. Field observations and flume experiments on the nature of comet marks. Sediment. Geol. 26, 233–262.

White, M., 2001. Hydrography and physical dynamics at the NE Atlantic margin that influence the deep water cold coral reef ecosystem. EU ACES-ECOMOUND internal report, Department of Oceanography, NUI, Galway, 31 pp.

Young, I.T., Gerbrands J.J., Van Vliet L.J., 1995. Fundamentals of Image Processing. PH Publications, Delft, 110 pp.